

UNIVERSIDAD DE LOS ANDES

FACULTY OF SCIENCE

PHYSICS DEPARTMENT



**Phenomenological Study of  
Heavy Neutrinos at the LHC,  
through high mass resonances,  
using the vector boson fusion  
technique**

AUTHOR:

CARLOS MIGUEL PATIÑO

ADVISOR: CARLOS ANDRÉS FLÓREZ

BOGOTÁ D.C.

2017

# Contents

|          |                                    |           |
|----------|------------------------------------|-----------|
| <b>1</b> | <b>Introduction</b>                | <b>1</b>  |
| <b>2</b> | <b>Objectives</b>                  | <b>6</b>  |
| 2.1      | General Objectives . . . . .       | 6         |
| 2.2      | Specific Objectives . . . . .      | 6         |
| <b>3</b> | <b>Computational Resources</b>     | <b>7</b>  |
| <b>4</b> | <b>Signal Simulation</b>           | <b>9</b>  |
| <b>5</b> | <b>Definitions</b>                 | <b>12</b> |
| 5.1      | Variable Definitions . . . . .     | 12        |
| 5.2      | Cut Definitions . . . . .          | 13        |
| <b>6</b> | <b>Distribution Analysis</b>       | <b>15</b> |
| 6.1      | Normalized Distributions . . . . . | 15        |

# List of Figures

|     |  |    |
|-----|--|----|
| 1.1 | Feynman diagram of heavy neutrino production. (Taken from [8]) . . . . . | 3  |
| 1.2 | Feynman diagram of VBF process. . . . .                                  | 4  |
| 4.1 | MadGraph commands used to generate signal . . . . .                      | 9  |
| 4.2 | Feynman diagram of simulated process involving Z boson                   | 10 |
| 4.3 | Feynman diagram of simulated process involving photon                    | 11 |
| 6.1 | Unit plot of $\eta$ from the sub-leading $\tau$ with no cuts . . .       | 16 |
| 6.2 | Unit plot of $p_T$ of leading $\tau$ with no cuts . . . . .              | 17 |
| 6.3 | $p_T$ unit plots for different bodies in the event . . . . .             | 18 |
| 6.4 | Unit plot of $H_T$ with no cuts . . . . .                                | 19 |
| 6.5 | Unit plot of $S_T$ with no cuts . . . . .                                | 20 |

# Chapter 1

## Introduction

The standard model (SM) gathers the entire understanding about fundamental particles and their interactions. Although the model has successfully explained various physical phenomena observed experimentally, there are still multiple unanswered questions concerning particle physics. For example, experiments [1] have shown that accelerator and reactor, solar, and atmospheric neutrinos have mass by proving the existence of neutrino oscillations. The fact that there are neutrino oscillations contradicts the SM, because this model predicts that the neutrinos are massless. Some specific experiments for each neutrino category are: Super-Kamiokande [2] for solar and atmospheric neutrino oscillations, KamLAND [3] for reactor neutrinos, and K2K [4] for accelerator neutrino oscillations [5]. An additional open question about neutrinos is the fact that only neutrinos with left helicity have been observed. Helicity is defined as the projection of the particle's momentum vector over its spin direction. Only neutrinos with spin anti-parallel to its linear momentum have been observed.

In order to provide neutrinos with mass, several theories that extend the predictions of the SM have been proposed. One of the most known models is the "see-saw" or balance mechanism [6]. The see-saw mechanism includes three sub-models that provide mass to neutrinos. In this model,  $\Phi = (\phi^+, \phi^0)^T$  is the doublet associated with the SM Higgs Boson and  $L_l$  the representation of a doublet field associated with the lepton number +1. In the type I see-saw mechanism the product be-

tween  $L_l$  and  $\Phi$  results in a fermionic singlet state. In the type II see-saw mechanism, the product between the two elements forms a scalar triplet. Finally, the product between  $L_l$  and  $\Phi$  in the type III sub-model results in a fermionic triplet state. Besides the see-saw mechanism, other models propose the existence of neutrinos with high mass and right helicity. If this kind of neutrinos are observed, the left and right symmetry in the SM would be restored and the mechanism by which the neutrinos acquire mass would be explained.

Heavy neutrinos searches have been conducted in experiments LEP [7], CMS and ATLAS [8], but none of these collaborations has proved that heavy neutrinos exist. In order to understand heavy neutrino searches it is necessary to define the concept of jet. A jet at phenomenological level is defined as a quark or a gluon. In high energies experimental physics, a jet is defined as a collection of particles resulting from the fragmentation of quarks or gluons. Searches at CMS and ATLAS have focused in final states with associated leptons and jets. Figure 1.1 shows a Feynman diagram of the production of a heavy neutrino mediated by a W boson with left or right helicity. The final state for this process has two leptons ( $\mu$  or  $\tau$ ) and two jets.

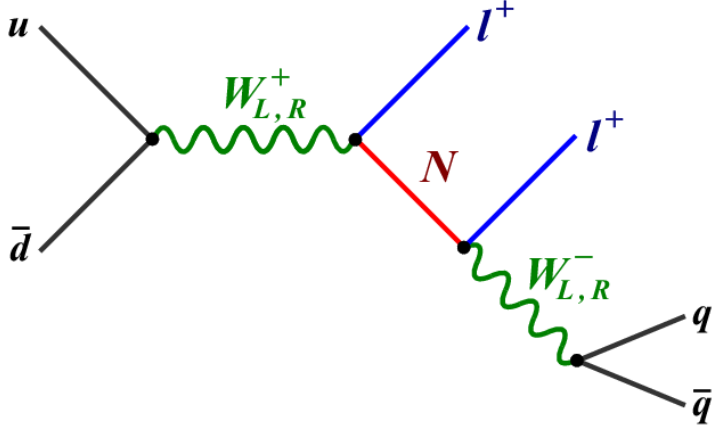


Figure 1.1: Feynman diagram of heavy neutrino production. (Taken from [8])

The main objective of this monograph is to perform a phenomenological study about the feasibility of conducting an experimental analysis for the detection of heavy neutrinos in the Large Hadron Collider (LHC) using a technique known as vector boson fusion (VBF). This technique has been recently used in the LHC [9] in searches for new physics. In high energy physics, the bosons  $W^{\pm}$ ,  $Z^0$  and  $\gamma$  are known as vector bosons. The process of vector boson fusion occurs through an electroweak interaction of associated quarks with the LHC proton beams. In the analysis, the production of heavy neutrinos is considered through the decay of a high mass hypothetical resonance known as  $Z'$  (shown in the Feynman diagram of Figure 1.2). This high mass resonance comes from the vector boson fusion process.

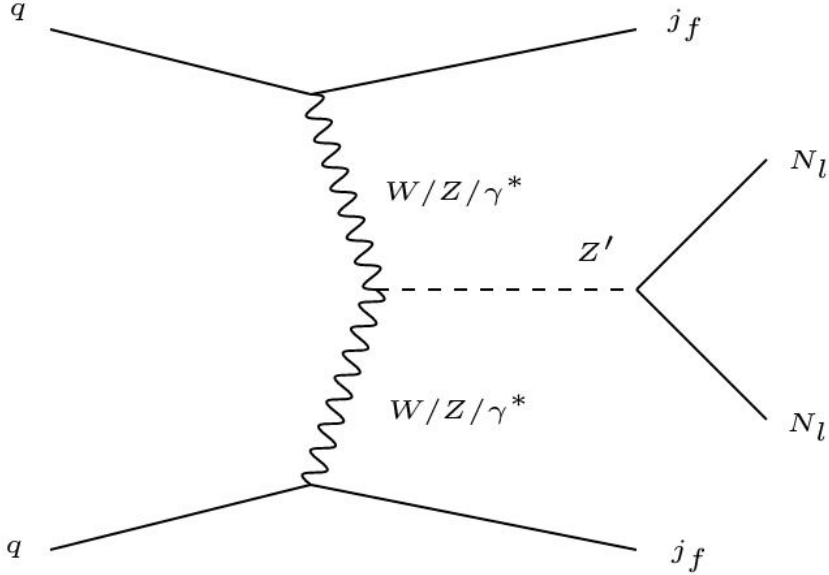


Figure 1.2: Feynman diagram of VBF process.

The production of the heavy neutrino consists in the interaction of two quarks associated to the protons colliding in the beam. The protons emit vector bosons that produce a heavy resonance when they fuse. The heavy resonance decays afterwards producing the heavy neutrinos ( $N_l$ ):  $pp \rightarrow jjZ' \rightarrow jjN_lN_l$ .

The VBF topology consists in requiring two highly energetic jets in the longitudinal region of the detector and in opposite hemispheres thereof. It has been shown that by requiring this type of event, the noise level (background) is reduced considerably in regions of difficult study in searches of new physics.

In order to conduct the analysis, it is important to simulate signal and background processes and to perform a detailed physical study of the variables that allow to distinguish signal for experimental noise. It is necessary to use a quantitative estimator commonly known as figure of merit to determine optimal cuts in the mentioned variables. The

latter with the objective of reducing the amount of experimental noise by finding the optimal cuts in the relevant variables. For this particular analysis, the significance formula that will be used is the one shown in Equation 1, where  $S$  is the significance,  $N(s)$  is the number of signal events, and  $N(B)$  is the number of background events.

$$S = \frac{N(s)}{\sqrt{N(s) + N(B)}} \quad (1.1)$$

Furthermore, it is important to establish the expected experimental sensitivity using maximum likelihood limits or the calculation of the final significance for different hypothetical signal points. The procedure described would allow to conclude whether a study for the detection of heavy neutrinos at the LHC is feasible or not.



# Chapter 2

## Objectives

### 2.1 General Objectives

Conduct a phenomenological study to determine the possible experimental sensitivity of heavy neutrino searches in the LHC, using the VBF topology, in channels with high-mass resonance production.

### 2.2 Specific Objectives

- Develop the signal events and experimental noise simulations using MadGraph, Pythia, and Delphes software.
- Write an analysis code using ROOT software to analyze the simulated data.
- Conduct a physical study of the appropriate cinematic and topological variables that show strong separation between signal and background.
- Find the optimal cut points of the relevant physical variables using a significance figure.
- Conduct a statical analysis of the results.

## Chapter 3

# Computational Resources

The project requires computational work, because simulations of events from the different processes are needed. Also, an analysis of the samples using the analysis code is required. The background and signal samples will be simulated using the software MadGraph [10], Pythia [11] and Delphes [12]. The data analysis and all the subsequent cinematic, topological, and optimal cuts analyses will be performed using ROOT software [13].

Pythia is a software that allows the simulation of various strong processes models that evolve from a few bodies to final states with high particle multiplicity. Particularly, in this case Pythia will be used for the simulation of quark and gluon fragmentation processes. This fragmentation process occurs when, due to an intrinsic characteristic of the strong interaction, there is an energy gain caused by the increase of the distance of two bound quarks. If the separation is enough to reach a critical energy, a pair quark-antiquark is created. The Pythia simulation is necessary, because processes like the ones mentioned above occur during a proton collision at the LHC.

MadGraph is an event generator software that allows the simulation of collision between two particle beams. For this analysis in particular, the simulations will consist in proton collision at 13 TeV in order to reproduce the actual conditions of the LHC. MadGraph includes the physical parameters that determine the production probability of a given process, as well as the possible decays that the initial simulated

particles suffer. Besides providing the necessary matrices to calculate the cross sections of the processes, MadGraph also creates the pictorial representations of the Feynman Diagrams from the generated processes. To this end, the software uses perturbation theory in the calculations of production and generation of physical processes.

Delphes is a software used to add the effects that a multipurpose detector, like ATLAS or CMS, may have on the particles to the Monte Carlo simulations performed for different processes. In this particular case, Delphes is necessary to simulate the interaction of the particles coming from the generated processes in MadGraph and Pythia with the CMS components. Namely, reproducing the conditions of the detector and the uncertainties coming from the measuring process is achieved by using Delphes. The changes in the cinematic variables due to their interaction with matter, errors caused by the electronics of the detector, and the additional particles generated because of the interaction between the particles and the detector components can be accounted for using Delphes. Other functionalities included in Delphes are: simulation of the detector geometry, the effect of the magnetic field over the particles, and the particle identification and reconstruction efficiencies, among others.

ROOT is a software library developed by CERN to perform data analyses related with particle physics. One of the main characteristics of this library is the possibility of handling large volumes of data efficiently. The latter is achieved by using a tree structure in which the information related with the particles is stored and can be accessed easily using ROOT functionalities. Other features included in the library are the creation of histograms from data trees, multivariate analysis, four-vector calculations, among others. By using ROOT functionalities, it is also possible to estimate optimal cuts in variables to reduce experimental noise to its minimum. This is why the entire final analysis will involve using tools provided by ROOT.

## Chapter 4

# Signal Simulation

The MadGraph signal simulation was performed assuming that the mass of the heavy neutrino was 1.5 TeV. Also, taking into the account that the analysis was going to be performed using Vector Boson Fusion, the parameter of minimum pseudorapidity separation ( $\Delta\eta$ ) between two jets was set to 3.5.

The commands used to generate the desired signal were the ones shown in Figure 4.1.

- `import model SM_HeavyN_NLO`
- `generate p p > n3 ta+ j j QCD=0, n3 > ta+ j j`
- `add process p p > n3 ta- j j QCD=0, n3 > ta- j j`
- `add process p p > n3 ta+ j j QCD=0, n3 > ta- j j`
- `add process p p > n3 ta- j j QCD=0, n3 > ta- j j`

Figure 4.1: MadGraph commands used to generate signal

The first command imports the theoretical model that includes the interactions related with the heavy neutrino formation and decay. The

next command specifies the processes that are going to be simulated.  $pp > n3 \tau^+ jj$  stands for the proton-proton collision that decays into a heavy neutrino, a  $\tau$  with positive charge, and two jets. The flag  $QCD=0$  is used to exclude all strong interactions that can be involved in the process. Finally,  $n3 > \tau^+ jj$  is used to force the decay of the heavy neutrino into a  $\tau$  charge positively and two jets. The subsequent commands are used to take into account all the possible combinations of the electrical charge that the  $\tau$  may have.

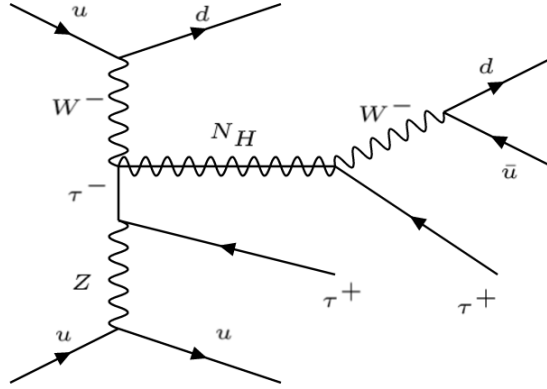


Figure 4.2: Feynman diagram of simulated process involving Z boson

Figures 4.2 and 4.3 show two of the main possible diagrams generated by MadGraph for the processes simulated. These two diagrams present a complete picture involving the processes shown in the diagrams of Figures 1.2 and 1.1. Figure 1.2 shows the diagram of the vector boson fusion process, occurring in Figures 4.2 and 4.3 in the fusion of the W boson with the Z boson and the photon ( $\gamma$ ) respectively. In these last two diagrams, the decay of the W boson coincides with the one shown in Figure 1.1 for the decay of the W boson resulting in a heavy neutrino and a lepton, which in this case is a  $\tau$ .

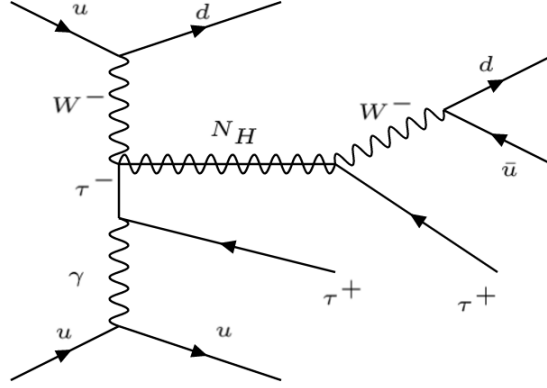


Figure 4.3: Feynman diagram of simulated process involving photon

The simulation was performed in 10 different simulation batches each one containing 10,000 events. Every batch was generated with a different random seed to guarantee the independence of the events between each one of the generated batches. This independence was necessary because the 10,000 event files were merged to form a single file with 100,000 events. As explained earlier, after the events were simulated in MadGraph they were passed to Pythia and then to Delphes so the signal resembled one that could be found at CMS.

# Chapter 5

## Definitions

### 5.1 Variable Definitions

The transverse momentum or  $p_T$ , is defined as the momentum component that a particle has in the plane perpendicular to the beam line. In the coordinate system of the LHC, this plane corresponds to the  $x - y$  plane.

The variable related with the polar angle in the LHC is called pseudorapidity, or  $\eta$ , defined as in Equation 5.1. The use of this variable is justified for mainly two reasons. The first one is that  $\Delta\eta$ , contrary to  $\Delta\theta$ , is a Lorentz invariant. This makes  $\Delta\eta$  a more natural variable than  $\Delta\theta$  for relativistic calculations. The second reason is that the distribution of the values of  $\eta$  in barrel region, where the multiplicity of particle is less than in the end-caps, is wider allowing the  $\eta$  particle distribution to be approximately constant.

$$\eta = -\ln \left[ \tan \left( \frac{\theta}{2} \right) \right] \quad (5.1)$$

In each event, a maximum of six jets that had a  $p_T$  greater than 15 GeV and its absolute value of  $\eta$  less than 5.0 were stored to be analyzed later. Among this list of jets, the two jets whose summed masses resulted in the greatest mass combination were stored and defined as the Di-Jet Pair. The jet with greater momentum in the Di-Jet Pair is the leading jet and the other one in the pair is the sub-leading jet. Another variable

defined regarding the Di-Jet Pair was the Di-Jet mass and corresponds to the sum of the masses from the jets in the Di-Jet Pair.

With the idea of exploiting the possible difference between signal and background in the  $p_T$  for jets and  $\tau$ 's, two new variables shown in Equations 5.2 and 5.3 were defined to check for possible further separation between signal and background. As shown in equation 5.2, the  $H_T$  variable is defined as the scalar sum of the jets with  $p_T$  greater than 30 GeV and  $|\eta| < 5$  that are not B-jets and that are not the jets in the Di-Jet Pair.  $S_T$  is defined as the scalar sum of jets that fulfill the same conditions of  $H_T$ , added to the  $p_T$  of the  $\tau$ 's in the event.

Since the  $\tau$  selection is important for this analysis, it is relevant to provide a further description of the selection criteria for the  $\tau$ 's in the simulated events. For starters, a jet identified as a tau is considered a valid  $\tau$  if it has a transverse momentum greater than 20 GeV. Also, it was required that a valid  $\tau$  should not overlap with an electron or a muon. That is, the  $\Delta R$ , defined as  $\Delta R = \sqrt{(\Delta\eta)^2 + (\Delta\phi)^2}$ , should not be less than 0.3. This condition guarantees that the jet identified as a  $\tau$  does not overlap with other leptons. Since the final state for this analysis includes two  $\tau$ 's, the two taus with greater  $p_T$  are selected among a maximum of three taus stored for each event. The leading  $\tau$  is the one with highest  $p_T$  and the sub-leading  $\tau$  is the one with second highest  $p_T$ .

$$H_T = \sum_{i=1}^n p_T(jet_i) \quad (5.2)$$

$$S_T = \sum_{i=1}^n p_T(jet_i) + \sum_{j=1}^m p_T(\tau_j) \quad (5.3)$$

## 5.2 Cut Definitions

In order to achieve a separation between background and signal, several successive requirements for the variables of the particles in the event were made. These requirements are defined as cuts, and for each cut the events that do not comply with the established condition are not taken into account to fill the histograms. Eight cuts were made to the



histograms, storing in each cut the resulting distributions to analyze them later. The first four cuts were related with the jets and  $\tau$ 's in the event, and the subsequent four were related with the VBF topology. In the next paragraphs of this section a description of each one of the cuts is given as well as the order in which they were performed.

The first cuts that were made to the histograms were required that the leading and sub-leading  $\tau$ 's should have a minimum transverse momentum of 20 GeV and a maximum of 2.1 for the absolute value of  $\eta$ . The second cut guarantees that the  $\tau$ 's left are detected by the barrel and not the end-caps of the detector. That is an important condition, because the detection components in the barrel section are more accurate than the ones in the end-caps. As a result, a signal detected in the barrel is most certain to be accurate than one detected in an end-cap.

The next cut requires that the event does not have any B-jet. This cut is justified by the fact that one of the main backgrounds for the signal is the top anti-top ( $t\bar{t}$ ) process. The interaction between the top and anti-top quark is related with the production of jets associated with the  $b$  quark or B-jets. That is why, much of the  $t\bar{t}$  should be eliminated by requiring no B-jets in the event. This fact will be later analyzed further in chapter 6. The cut that follows the one regarding the B-jets selects the events that have a minimum of two jets with transverse momentum greater than 30 GeV. These two jets must be different from the ones used in the Di-Jet Pair.

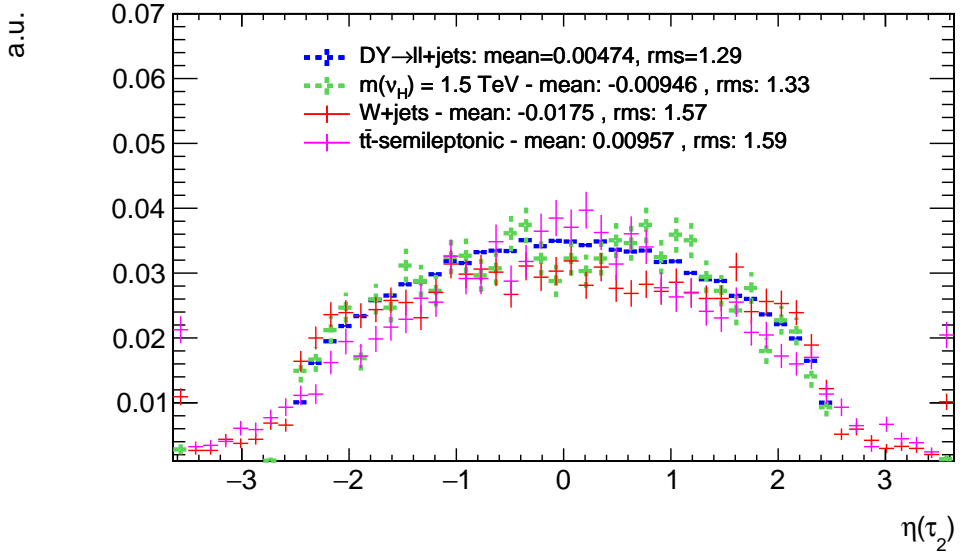
The last three cuts made to the histograms are related to the VBF topology. The first of the three selects events in which the product of  $\eta$  from the leading and sub-leading jets is negative. This condition guarantees that the jets in the Di-Jet Pair are in opposite hemispheres. The next cut requires that the leading and sub-leading jets of the event have a  $\Delta R$ , defined earlier in this section, greater than 3.8. Finally, the last cut requires that the Di-Jet mass of the event is greater than 500 GeV.

## Chapter 6

# Distribution Analysis

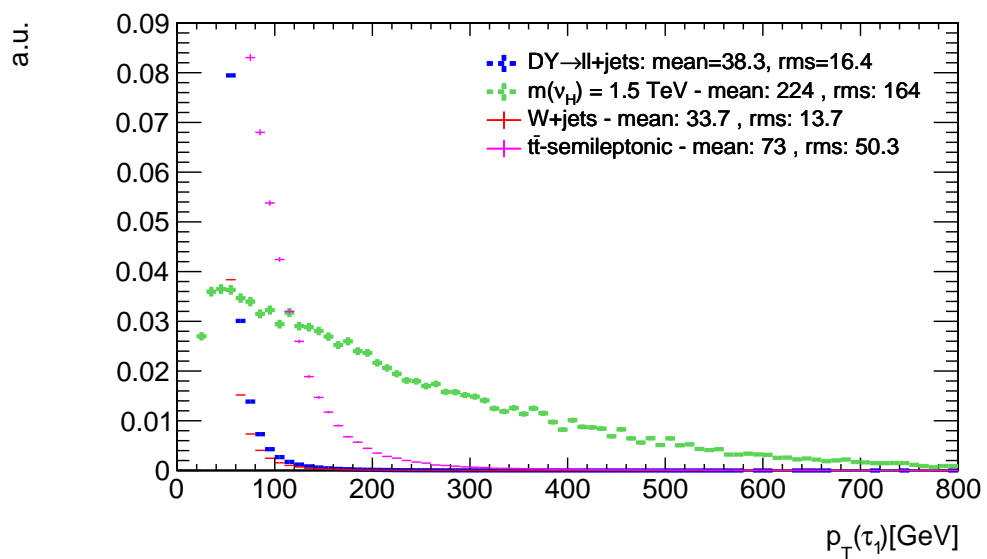
### 6.1 Normalized Distributions

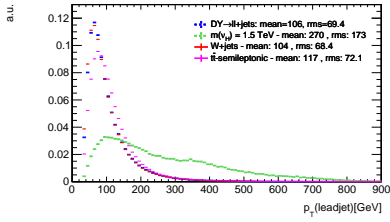
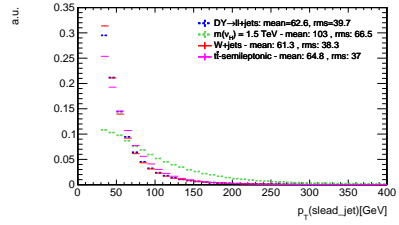
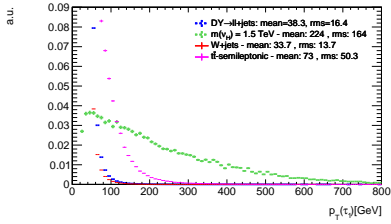
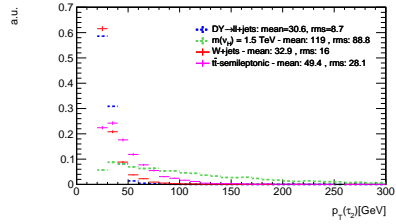
The normalized plots are useful to check the shape of backgrounds and signal distributions. These shapes help to identify which variables are not useful for the analysis because the backgrounds overlap with the signal and which variables have to be studied with greater detail because the signal separates from the backgrounds from certain points. An example for both cases is provided in Figures 6.1 and 6.2. In figure 6.1 it can be seen that the signal overlaps for all values with the background distributions. That is why this plot can be used to conclude that the  $\eta$  variable from the sub-leading  $\tau$  is not useful to isolate the signal from the background. In contrast, the plot in Figure 6.2 show that from around 150 GeV the signal separates from the background distributions. This separation for the  $p_T$  of the leading  $\tau$  suggests that this variable should be examined more closely through the subsequent cuts.

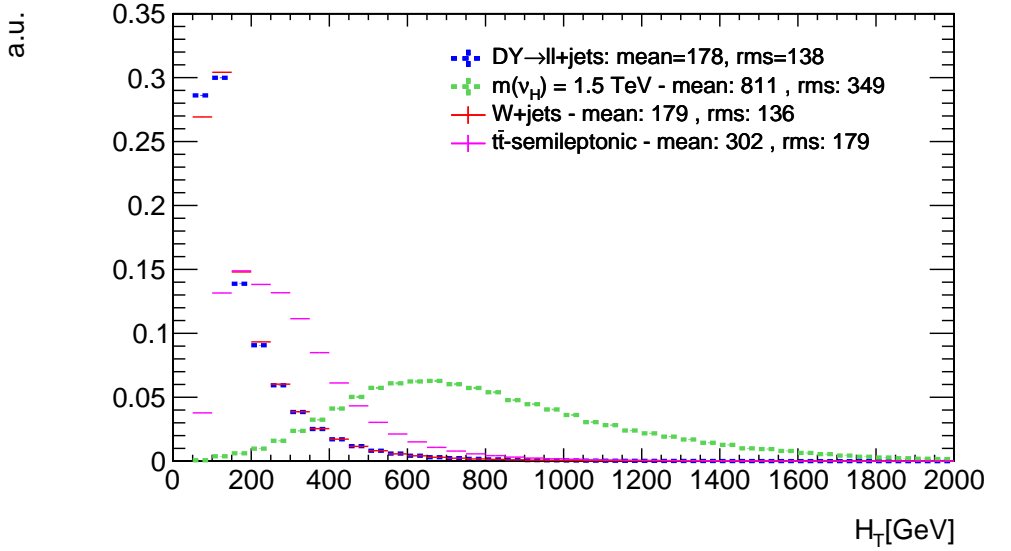
Figure 6.1: Unit plot of  $\eta$  from the sub-leading  $\tau$  with no cuts

To understand the definition of  $H_T$  and  $S_T$  mentioned in chapter 5, the plots in Figure 6.3 are shown. The four plots show a separation, in some cases a smaller than others, between the signal and backgrounds distributions. Although the normalized graphics from the jets correspond to the ones of the Di-Jet Pair, that as mentioned in chapter 5 were not taken into account in  $H_T$  and  $S_T$ , a tendency of the signal jets to have greater transverse momentum than the ones in the backgrounds is shown. This tendency is also displayed for both  $\tau$ 's. Hence, the distributions of  $H_T$  and  $S_T$  should show a similar behaviour because this variables are the result of adding the transverse momentum of jets and  $\tau$ 's in the event.

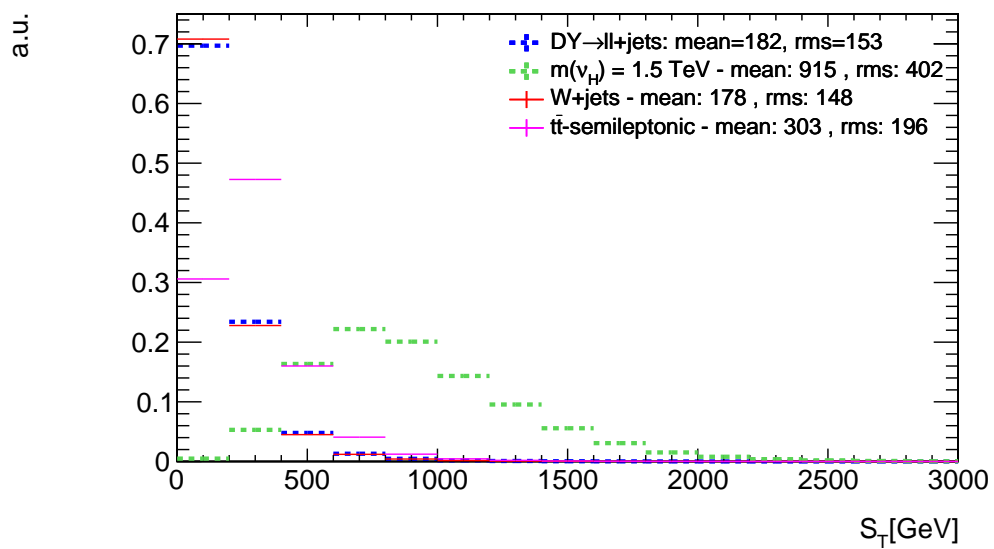
In Figures 6.4 and 6.5, the normalized plots with no cuts of  $H_T$  and  $S_T$  are shown. It can be seen that indeed a greater separation between signal and background was achieved. Unlike the distributions of the  $\tau$ 's and jets transverse momentum, the maxima of  $H_T$  and  $S_T$  lie outside the backgrounds distributions. Furthermore, the background that overlaps at a greater energy with the signal corresponds to  $t\bar{t}$ .

Figure 6.2: Unit plot of  $p_T$  of leading  $\tau$  with no cuts

(a) Leading jet  $p_T$  unit plot(b) Sub-leading jet  $p_T$  unit plot(c) Leading  $\tau$   $p_T$  unit plot(d) Sub-leading  $\tau$   $p_T$  unit plotFigure 6.3:  $p_T$  unit plots for different bodies in the event

Figure 6.4: Unit plot of  $H_T$  with no cuts

Taking into account what was mentioned in section 5.2, the overlap between the signal and this background could be reduced with the cut related with the number of B-jets in the event. This is why this two variables need to be studied closer in the analysis.

Figure 6.5: Unit plot of  $S_T$  with no cuts

# Bibliography

- [1] Particle Data Group, Olive, K. A. et al. , Chin.Phys. C38, 090001 (2014)
- [2] Fukuda, S. et al. (2003) Nuclear Instruments and Methods in Physics Research A 501 (2003) 418–462
- [3] Decowski, M. (2016). KamLAND’s precision neutrino oscillation measurements. Nuclear Physics B, 908, pp.52-61.
- [4] K2K Collaboration: Aliu, E. et al (2005). Evidence for Muon Neutrino Oscillation in an Accelerator-Based Experiment. Physical Review Letters, 94(8).
- [5] Nakamura, K. et al. (2010) (Particle Data Group), J. Phys. G 37, 075021 (2010)
- [6] Deppisch, F., Bhupal Dev, P., & Pilaftsis, A. (2015). Neutrinos and collider physics. New Journal Of Physics, 17(7), 075019. <http://dx.doi.org/10.1088/1367-2630/17/7/075019>
- [7] Abdesslam, A. et al. (2014) Type II Seesaw Higgsology and LEP/LHC constraints. arXiv:1411.5645 [hep-ph]
- [8] Khachatryan, V., Sirunyan, A., Tumasyan, A., Adam, W., Asilar, E., & Bergauer, T. et al. (2016). Search for heavy Majorana neutrinos in  $e \pm e \pm + \text{jets}$  and  $e \pm \mu \pm + \text{jets}$  events in proton-proton collisions at  $s = 8 \sqrt{s} = 8 \text{ TeV}$ . Journal Of High Energy Physics, 2016(4).



- [9] Brooke, J., Buckley, M., Dunne, P., Penning, B., Tamanas, J., & Zgubič, M. (2016). Vector boson fusion searches for dark matter at the LHC. *Physical Review D*, 93(11). <http://dx.doi.org/10.1103/physrevd.93.113013>
- [10] Alwall, J., Herquet, M., Maltoni, F., Mattelaer, O., & Stelzer, T. (2011). MadGraph 5: going beyond. *Journal Of High Energy Physics*, 2011(6). [http://dx.doi.org/10.1007/jhep06\(2011\)128](http://dx.doi.org/10.1007/jhep06(2011)128)
- [11] Sjöstrand, T., Ask, S., Christiansen, J., Corke, R., Desai, N., & Ilten, P. et al. (2015). An introduction to PYTHIA 8.2. *Computer Physics Communications*, 191, 159-177. <http://dx.doi.org/10.1016/j.cpc.2015.01.024>
- [12] de Favereau, J., Delaere, C., Demin, P., Giammanco, A., Lemaître, V., Mertens, A., & Selvaggi, M. (2014). DELPHES 3: a modular framework for fast simulation of a generic collider experiment. *Journal Of High Energy Physics*, 2014(2). [http://dx.doi.org/10.1007/jhep02\(2014\)057](http://dx.doi.org/10.1007/jhep02(2014)057)
- [13] Antcheva, I., Ballintijn, M., Bellenot, B., Biskup, M., Brun, R., & Buncic, N. et al. (2009). ROOT — A C++ framework for petabyte data storage, statistical analysis and visualization.